CIRP Journal of Manufacturing Science and Technology 47 (2023) 168–183

Contents lists available at ScienceDirect

CIRP Journal of Manufacturing Science and Technology

journal homepage: www.elsevier.com/locate/cirpj

Analysis and development of elliptical tool path in trochoidal milling

Mohamed Wagih [a,b], Ibrahem Maher [a,c], Hassan El-Hofy [d], Jiwang Yan [e], Mohsen A. Hassan [f,g,*]

[a] Department of Industrial and Manufacturing Engineering, Egypt-Japan University of Science and Technology, Alexandria 21934, Egypt
[b] Design and Production Department, Faculty of Engineering, Ain Shams University, Cairo 11566, Egypt
[c] Department of Mechanical Engineering, Faculty of Engineering, Kafrelsheikh University, Kafrelsheikh 33516, Egypt
[d] Production Engineering Department, Faculty of Engineering, Alexandria University, Alexandria 21544, Egypt
[e] Department of Mechanical Engineering, Faculty of Science and Technology, Keio University, Yokohama 223-8522, Japan
[f] Materials Science and Engineering Program, School of Innovative Design Engineering, Egypt-Japan University of Science and Technology, Alexandria 21934, Egypt
[g] Mechanical Engineering Department, Faculty of Engineering, Assiut University, Assiut 71516, Egypt

A R T I C L E I N F O

Keywords:
Trochoidal milling
Cutting forces
Material removal rate
Surface roughness
Elliptical tool path

A B S T R A C T

Trochoidal milling has been developed to extend the cutting tool life as compared to conventional milling. It is widely used in the machining of slots and corners of molds and dies. There are several tool paths typically used in trochoidal milling such as true, circular, variable-feed, and variable-step trochoidal tool paths. However, these paths suffer from low material removal rates, low surface qualities, high CPU processing times, and/or the requirement of high-dynamic machine tools. Elliptical trochoidal tool path showed its capability to improve the material removal rate, but the expected low surface quality of the produced slot. In this paper, the elliptical tool path will be analyzed analytically and experimentally. The effect of elliptical tool path on material removal rate, cutting forces, walls waviness, and surface roughness have been investigated. A novel linear elliptical-based tool path has been proposed to enhance the elliptical tool path performance by improving both material removal rate and surface quality. A Performance index has been utilized to evaluate the performance of these processes. An analytical model for the local maximum chip thickness in elliptical tool path has been conducted to correlate this path with the cutting forces. The slot walls waviness has been modeled based on the cutting tool path geometry and validated experimentally with error less than 11%. The experimental results showed that the elliptical tool path improved the material removal rate by 11%, with a slight reduction in the maximum resultant cutting force by 3%. On the other hand, the walls waviness and surface roughness have been increased by 45% and 38% respectively as compared to the typical true trochoidal tool path. The introduction of linear paths at the elliptical path sides in the linear-elliptical tool path improved the performance index about 18 times by improving the material removal rate, waviness, and surface quality by 5%, 300%, and 74% respectively, without a significant effect on cutting forces. Therefore, the novel linear-elliptical paths are promising tool paths in increasing the performance of trochoidal milling due to the improved material removal rate, walls waviness, and surface quality, without a significant effect on cutting forces, which will improve the process machinability and cost-effectiveness.

1. Introduction

Recently, machine tools and cutting tools have been rapidly developed, improving productivity and production rates. Accordingly, new machining techniques have been developed to utilize these advancements effectively, such as high-speed, high-feed, and high-performance machining processes. On the other hand, undesired consequences have been revealed such as the increase of cutting tool temperature and wear, cutting forces, and surface roughness. In order to overcome these effects, optimization of the process and tool parameters have been achieved, in addition to developing new techniques. In milling, advanced techniques have been developed, such as trochoidal milling, plunge milling, helical milling, laser-assisted milling, etc. [1,2].

Trochoidal milling, Fig. 1, is a milling process that has been developed to extend the cutting tool life by reducing the cutting tool temperature. In this process, a rotating cutting tool, with a rotational speed

* Corresponding author at: Materials Science and Engineering Program, School of Innovative Design Engineering, Egypt-Japan University of Science and Technology, Alexandria 21934, Egypt.
E-mail address: mohsen.khozami@ejust.edu.eg (M.A. Hassan).

https://doi.org/10.1016/j.cirpj.2023.10.002
Received 28 March 2023; Received in revised form 10 October 2023; Accepted 11 October 2023
1755-5817/

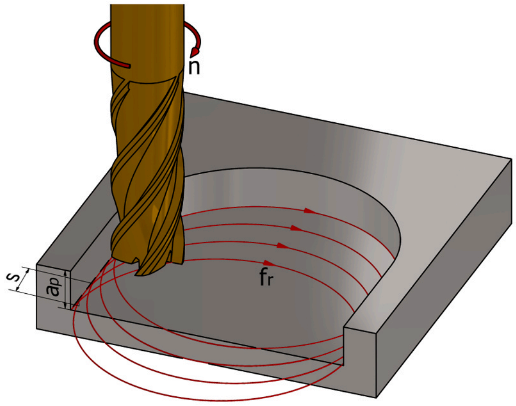

Fig. 1. Schematic drawing of the trochoidal milling process.

n, set at an axial depth of cut a_p, moves in a definite path with a feed rate f_r. The material removal is performed only in the first half of the tool revolution, while the tool is cooled down in the second half. This process kinematics allows the increase of tool cooling time, in addition to the use of a tool of diameter less than the machined slot width. Because of this enhanced tool cooling mechanism, the tool life is longer as compared to conventional milling, and the cooling fluid may not be used, hence the process is more effective economically and environmentally. The tool path can be either continuous or discontinuous. In the continuous tool path, the tool follows a true trochoidal path, Fig. 2 **(a)**, while in the discontinuous path, Fig. 2 **(b)**, the tool passes in a circular path and then advances a distance, defined as trochoidal step, *s*, after each complete revolution. The continuous tool motion gives the tool more stability, but the tool path programming is more complex. While the discontinuous path is composed of two different paths: linear and circular, which are simpler in programming. The tool stability is less due to the sudden change in tool direction at the end of each portion.

The surface texture of the slot walls of the slot is one of the main trochoidal milling defects. Surface texture is concerned with the geometrical irregularities of the machined surface of the workpiece. It includes form deviation, waviness, roughness, lays, and flaws [1,31,32]. Structural deviations are irregularities of the first order due to systematic errors. Surface waviness is a second-order error in the machined surface that is caused by systematic or random influences. The surface roughness is irregularities of third up to sixth order that occurs because of the process effects, grains orientation, etc. Generally, all these deviations are superposed on a real surface. In order to separate roughness from waviness, filters are employed in the measurement process as recommended by ISO 4287. Fig. 3 demonstrates the superimposition of waviness and roughness on the surface of the workpiece. The waviness can be defined by the waviness spacing and waviness height (W). The surface roughness is separated from the waviness by considering the roughness measurements in a small distance known as the cut-off distance. The surface roughness parameters are the roughness spacing and its height. The surface roughness height can be defined by different parameters such as peak-to-valley height, R_z, arithmetic average height, R_a, root mean square, R_q, etc. [33]. The assessment of the cutting tool path facilitates the determination of this phenomenon.

In comparison to conventional milling, trochoidal milling is characterized by lower cutting temperature, tool wear, and cutting forces due to the lower engagement angle between tool and workpiece [3–6]. Therefore, it is efficient in the machining of difficult-to-cut materials such as Ti-6Al-4V, duplex stainless steel, Inconel superalloys, etc., and in high-speed machining [1,7–11]. During the cooling portion of the tool path, the tool does not perform any cutting, so the material removal rate is less as compared to conventional milling [4]. The discontinuity of the tool path results in higher surface roughness and lower dimensional accuracy [4,12]. Uddin et al. proved experimentally that trochoidal milling is suitable for machining deep and narrow grooves [13].

Several efforts have been exerted to improve the trochoidal milling process such as optimization of the process parameters, using variable process conditions, and developing the cutting tool path. Another perspective was to apply this process in difficult-to-cut conditions, such as the machining of difficult-to-cut materials, high-speed machining, and machining of corners. In the papers [5,6,14–17], it has been proved experimentally that during trochoidal milling, cutting forces, surface roughness and energy consumption can be reduced by decreasing the axial depth of cut, trochoidal step, or feed rate, however the lessening of material removal rate. Karkalos et al. showed the good influence of increasing the cutting speed on surface quality [15]. In order to reduce the process cycle time, M. Otkur and I. Lazoglu proposed double trochoidal milling, where the tool revolution direction is inverted after each cutting cycle [18]. Although the material removal rate has been improved by 50% as compared to conventional trochoidal milling, the cutting forces have been increased by the same ratio. Additionally, this technique reduced the tool cooling time and requires high machine tool dynamics, i.e., acceleration and jerk. For the same purpose, Salehi et al. developed a complicated tool path nominated as epicycloidal tool path [19]. In comparison to circular trochoidal tool path, the cycle time was less by 20% at the expense of a 10% increase in forces. Oh et al. proved that laser assistance in trochoidal milling has a great impact on the reduction of cutting forces and specific energy by 100% and 20% respectively [20]. Huang et al. proposed an elliptical trochoidal tool path of 0.5 aspect ratio, as an alternative to the typical circular trochoidal tool path, to improve the material removal rate during groove machining [21]. By using this path, they succeeded in improving the material removal rate by 12.1% as compared to the typical tool path. They did not consider the effect of this path on surface quality and product accuracy. Jaco et al. proposed a new Bézier curve-based tool path technique and a new stochastic hill climbing algorithm-based optimization method to increase the material removal rate of trochoidal milling [22]. S. Hesterberg and B. Albert proved that variable-feed (dynamic) trochoidal milling is better than the static one in terms of forces, however, it requires high dynamics of the machine tool [23]. Recently, Hernández et al. showed the high performance of dynamic trochoidal milling in improving material removal rate and tool life as compared to the static one [24]. Waszczuk et al. concluded that the stretched trochoidal tool path can produce a better surface quality than that of circular trochoidal, true trochoidal, and semi-trochoidal paths [12]. Waszczuk et al. proved that surface roughness is significantly affected by the trochoidal tool path [12,25,26]. They proved that semi-quasi trochoidal milling produces the roughest surface in comparison to the other processes due to the sudden change of tool movement direction. They proved that adding linear paths to the sides of the

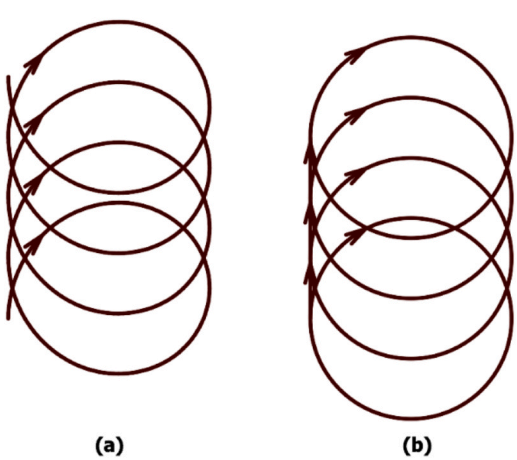

Fig. 2. Different types of trochoidal tool paths: (a) true trochoidal tool path, (b) circular-type trochoidal tool path.

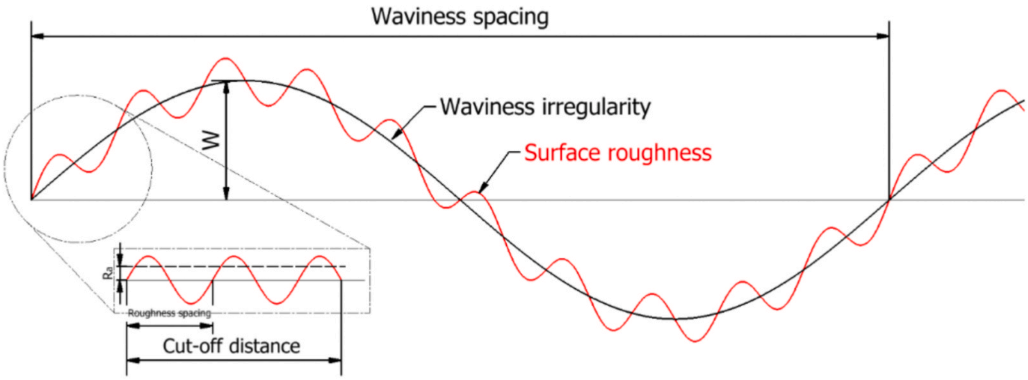

Fig. 3. Waviness and roughness parameters.

main trochoidal path enhances the surface roughness significantly.

Pockets include wide areas, slots, and corners. It has proved that the wide areas are better to be machined by contour-parallel milling technique, while slots and corners are better to be machined by trochoidal milling [13,27,28]. Cutting forces increase significantly at the corners where the engagement angle between tool and workpiece increases. Deng et al. developed an optimization approach for the trochoidal radius and step to maximize the material removal rate [29]. They built their model on the determination of the maximum engagement angle between tool and workpiece considering the limiting cutting force. However, the success of their technique requires a long time for path creation and simulation in CAM software. In addition, they did not consider the influence of this technique on product accuracy or quality. Wang et al. presented an adaptive trochoidal toolpath technique to reduce fluctuations in cutting forces along the tool path [27]. They used a variable step technique to control the cutting forces, which led to the reduction of tool path length and cutting forces, and tool life and material removal rate improvement. Wang et al. extended this technique to include two strategies: radius-varying trochoidal milling and contour-parallel toolpath to improve and stabilize cutting forces and material removal rate along the machined contour [28]. For the aim of simulation time reduction, Jasco et al. presented a fast algorithm to stabilize the engagement angle between tool and workpiece like pixel-based methods [30]. The tool path changes as the tool advances depending on the shape to be removed.

Although several research has been conducted to improve the trochoidal milling performance, they were either based on the enhancement of one factor only or constrained to machine tools of high dynamics. The elliptical tool path showed its effectiveness in the enhancement of material removal rate in trochoidal milling without affecting the cutting forces, but the tool suddenly changes its motion, which may harm the surface quality. Hence, analysis and development of this path is required. In this paper, the elliptical tool path will be analyzed theoretically and experimentally. A novel linear-elliptical trochoidal tool paths will be presented as an improvement of the elliptical tool path and an alternative to the typical true trochoidal tool path. The proposed tool path combines elliptical and linear motions of the cutting tool to improve both material removal and surface texture simultaneously.

The objective of this paper is to investigate the effects of elliptical tool path on material removal rate, surface texture, and performance index as compared to the typical trochoidal tool path. The performance index is an index that compromises the investigated responses in only one factor. In addition, the effects of the proposed linear-elliptical on surface texture and process performance will be studied.

The structure of this paper consists of six main sections. The introduction presents the significance of trochoidal milling process, the literature review of trochoidal milling, and the research gap. In the second section, the elliptical trochoidal tool path will be analyzed theoretically. The third section includes a description of the proposed linear-elliptical tool path and its significance. The fourth section provides the experimental work on elliptical and linear-elliptical tool paths. In the fifth section, results and discussion are presented. Finally, the paper results will be summarized in the conclusions sections.

2. Analysis of elliptical trochoidal tool path

This section presents an analysis of the elliptical tool path, including the study of the process kinematics, the tool path length, local maximum chip thickness, and walls waviness. MATLAB R2021b has been used in this analysis.

2.1. Elliptical tool path length

Fig. 4 illustrates the typical true trochoidal tool path (solid curve) and the elliptical tool path (dashed curve). Generally, the elliptical trochoidal tool path is characterized by a lower tool path length, but it is sharper on both sides as compared to the typical one. It can be described mathematically as in Eq. (1). The main parameters of this path are the lengths of the ellipse major diameter, *a,* and minor diameter, *b*, where

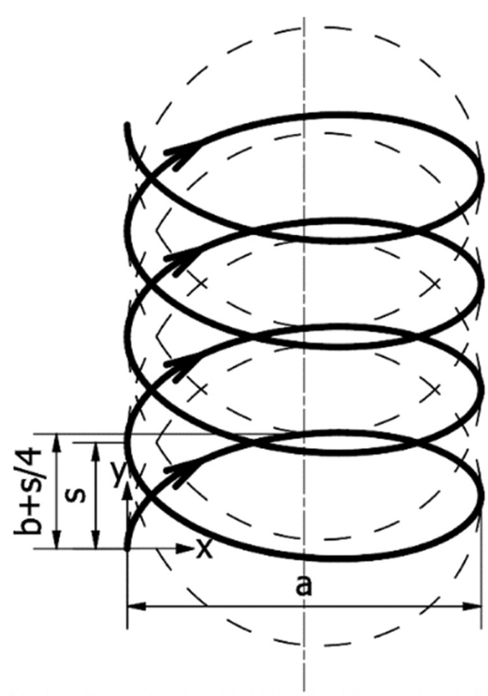

Fig. 4. The elliptical (solid curve) versus the circular (dashed curve) trochoidal tool paths.

the ratio between them is defined as the elliptical tool path aspect ratio, r_e, Eq. 2. Fig. 5 shows the correlation between the elliptical tool path aspect ratio, r_e, and the tool path length, L, at different slot widths, B. It can be revealed that the decrease in aspect ratio reduces the path length significantly. For all slot widths, by reducing the minor diameter length to half the major diameter length, i.e., $r_e = 0.5$, the tool path length is almost 23% less than that of the typical trochoidal path, $r_e = 1$. Therefore, the elliptical path has a great potential to be applied in trochoidal milling as it can enhance the material removal rate by reducing the tool path length. In this paper, the typical true trochoidal tool path, $r_e = 1$, will be nominated shortly as the circular tool path.

$$\begin{cases} x = -a\cos\theta \\ y = b\sin\theta + \dfrac{s\theta}{2\pi} \end{cases} \tag{1}$$

$$r_e = \frac{b}{a} \tag{2}$$

Where (a) is the elliptical path major diameter, (b) is the elliptical path minor diameter, (θ) is the tool center position angle, and (s) is the trochoidal step.

2.2. Local maximum chip thickness of elliptical trochoidal tool path

Altintaş and Lee proved that the tangential, radial, and axial cutting forces mainly depend on the chip thickness in addition to the coefficients of cutting forces [34]. Surface roughness, tool wear, cutting temperature, and other phenomena are affected by the cutting forces as well. Since the coefficients of cutting forces are dependent on the chip thickness, hence the local maximum chip thickness will be expressive for the cutting forces of elliptical trochoidal milling.

Fig. 6 illustrates the cutting tool (red circle) at two successive positions O_{C1} and O_{C2}, the elliptical tool center path C_1 (dashed line), the tool edge path during the previous revolution C_2, and the corresponding local maximum chip thickness, h_{max}. The distance between each two successive tool positions is the tool center feed per tooth, f_z. The elliptical tool center path C_1 is drawn based on Eq. (1) with the origin O_1, where the following path has the origin O_2. The tool edge path during the previous revolution C_2 is the offset curve of the tool path by the tool radius, R_t. It can be drawn based on Eq. (3). The maximum chip thickness at each position O_{C2}, located on C_1, can be calculated from Eq. (4). It depends on the coordinates of the points B (x_b, y_b) and D (x_d, y_d). Point B is the intersection point between the tool circle C_3 in position O_C, and the tool edge path during the previous revolution C_2. The coordinates of B can be determined by solving equations of these curves, **3** and **5**, simultaneously numerically. Point D is the intersection point between the tool in position O_C and line O_CB. The coordinates of D can be computed after the determination of point B as shown in Eq. (6).

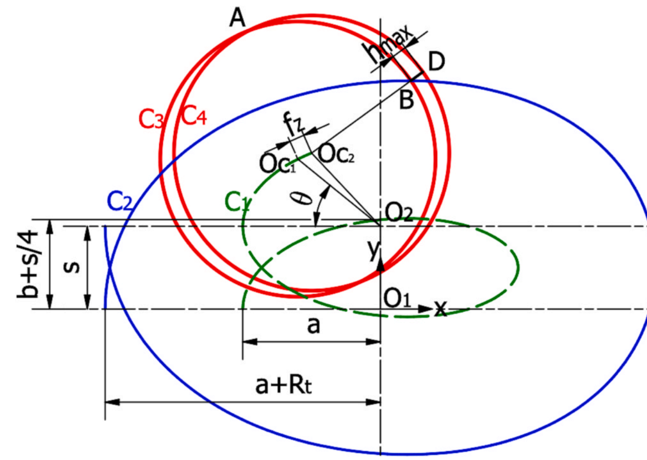

Fig. 6. Analysis of the elliptical tool path showing the maximum chip thickness, h_{max}.

$$\begin{cases} x_o = x_i + \left[\sqrt{\left(x_{O_{C_1}} - x_i\right)^2 + y^2_{O_{C_1}}} + R_t\right]\cos\left[\tan^{-1}\left(-\dfrac{dx}{dy}\right)\right] \\ y_o = \left[\sqrt{\left(x_{O_{C_1}} - x_i\right)^2 + y^2_{O_{C_1}}} + R_t\right]\cos\left[\tan^{-1}\left(-\dfrac{dx}{dy}\right)\right] \end{cases} \tag{3}$$

$$h_{\max} = \sqrt{(x_d - x_b)^2 + (y_d - y_b)^2} \tag{4}$$

$$\begin{cases} x_{C_3} = x_{O_{C_1}} + R_t\cos\theta \\ y_{C_3} = y_{O_{C_1}} + R_t\sin\theta \end{cases} \tag{5}$$

$$\begin{cases} x_d = x_{O_{C_2}} + R_t\cos\left[\tan^{-1}\left(\dfrac{y_b - y_{O_{C_2}}}{x_b - x_{O_{C_2}}}\right)\right] \\ y_d = R_t\cos\left[\tan^{-1}\left(\dfrac{y_b - y_{O_{C_2}}}{x_b - x_{O_{C_2}}}\right)\right] \end{cases} \tag{6}$$

Where (x_o, y_o) are the corresponding coordinates of the previous tool revolution curve C_2, (R_t) is the cutting tool radius, (x_i) is the x-intercept of the normal to the tool path C_1 at point $\left(x_{O_{C_1}}, y_{O_{C_1}}\right)$ with the x-axis, $\left(\frac{dy}{dx}\right)$ is the slope of the tangent to the tool path C_1 at the same point. $(h_{\max})$ is the local maximum chip thickness at the same point, (x_b, y_b) and (x_d, y_d) are the coordinates of the points B and D respectively, (θ) is angle where calculations take place; $\theta = [0, 2\pi]$, $\left(x_{O_{C_1}}, y_{O_{C_1}}\right)$ and $\left(x_{O_{C_2}},\right.$

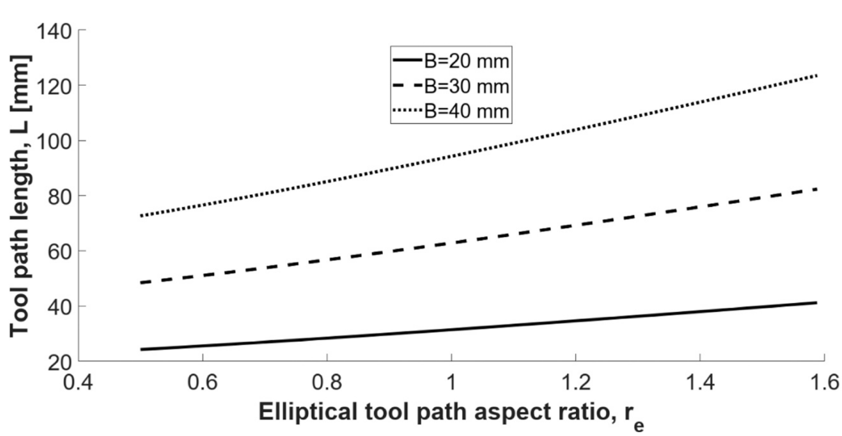

Fig. 5. The effect of elliptical tool path aspect ratio, r_e, on the tool path length, L, at different slot widths, B.

$y_{O_{C_2}}$) are center points of two successive arbitrary circles of radius R_t that lies on the tool path C_1, where the distance between them is the feed per tooth, f_z.

The variation of the local maximum chip thickness along the elliptical tool path is demonstrated in Fig. 7 for the aspect ratios 0.5–1.2 and the conditions in Table 1. Table 2 summarizes the figure highlights showing the maximum chip thickness value, h_{max}, the total cycle time, t_{cycle}, the time interval from the start of cutting to the maximum chip thickness, $t_{h_{max}}$, the tool cooling time interval, $t_{cooling}$, and the material removal rate at each aspect ratio. As the aspect ratio decreases from 1.1 to 0.6, the material removal rate increases significantly, and the maximum chip thickness is almost constant, but the cooling time reduces significantly. In addition, by reducing the aspect ratio, the maximum chip thickness is attained after a shorter time and kept constant for longer. By comparing the two elliptical tool paths of 0.5 and 1 aspect ratios, the material removal rate for the elliptical path of 0.5 aspect ratio is larger than that of the circular one by 21.8%, the maximum chip thickness is less by 5.9%, and the cooling time is less by 17.7%. Therefore, the material removal rate can be improved significantly without a significant effect on the chip thickness and consequently the cutting forces.

2.3. Slot walls waviness of elliptical trochoidal tool path

The large waviness of the slot walls is one of the trochoidal milling defects. It can be determined by considering the cutting tool path at the walls of the machined slot. Fig. 8 demonstrates the slot walls waviness due to the cutting tool motion in its path for the two types of trochoidal milling. The motion of cutting tool in a true trochoidal tool path, Fig. 8 **(a)**, produces waviness at both sides of the slot walls. In case of the circular-type trochoidal tool path, Fig. 8 **(b)**, the waviness is only at the right wall of the slot due to the cutting tool motion linearly on this side removing the unmachined fragments from the left wall. The waviness spacing for both paths and the elliptical-based tool paths is the trochoidal step, *s*, while its height, *W*, depends on the tool path, trochoidal step, trochoidal radius, and cutting tool radius. The waviness height at the right and left walls can be determined numerically by substituting s/2 in y_0 in Eq. (3) for the left wall and by s for the right one to find the value of x_0, hence the waviness can be calculated. Fig. 9 illustrates the effect of the elliptical path aspect ratio on the waviness of the slot left wall, W_l, and the waviness of the slot right wall, W_r. The increase of the elliptical tool path aspect ratio has a significant reducing effect on the waviness of both sides of the slot, enhancing the slot accuracy. Hence, the use of elliptical path has a negative effect on the slot walls waviness. In comparison to the circular path, r_e= 1, the use of elliptical path of 1.2 aspect ratio reduces the left and right walls waviness similarly by 18%, while the elliptical path of 0.6 aspect ratio produces higher waviness by 48%.

Table 1
Parameters used in the theoretical analysis of the elliptical and linear-elliptical tool paths.

Parameter	Value
Tool center feed rate, f_r [mm/min]	600
Trochoidal step, s [mm]	1
Rotational speed, n [rpm]	2000
Cutting tool diameter [mm]	10
Cutting tool number of teeth	4
Slot width [mm]	20

Table 2
Elliptical tool path maximum chip thickness, cycle time, and time interval till the maximum chip thickness for different aspect ratios.

r_e	h_{max} [mm]	t_{cycle} [s]	$t_{h_{max}}$ [s]	$t_{cooling}$ [s]	MRR [mm^3/min]
0.5	0.068	2.5	0.098	1.30	2879
0.6	0.062	2.6	0.132	1.35	2748
0.7	0.059	2.8	0.216	1.43	2608
0.8	0.057	2.9	0.424	1.50	2487
0.9	0.058	3.0	0.539	1.57	2367
1	0.059	3.2	0.694	1.64	2256
1.1	0.059	3.3	0.762	1.72	2154
1.2	0.060	3.5	0.766	1.80	2057

3. Linear-elliptical trochoidal tool path: a developed elliptical trochoidal tool path

Szalóki et al. [4] in addition to Waszczuk et al. [12] proved that conventional milling produces a better surface quality than that of trochoidal milling. This can be explained by the difference between the processes kinematics, as in trochoidal milling, the cutting tool suddenly changes its direction several times, increasing the produced vibrations at these locations. Waszczuk et al. proved that adding a linear motion to a stretched quasi-trochoidal path improved the surface quality by 60% [26].

In order to reduce the produced waviness and surface roughness at the slot walls due to the elliptical path, linear paths at the slot walls are suggested to be introduced through the elliptical tool path, forming a new path nominated as linear-elliptical tool path, Fig. 10. In this developed path, the tool moves forward a distance *d* from point *A* to point *B* in the linear path (1), followed by a forward elliptical path (2) from point *B* to point *C*. Thereafter, the tool travels backward a distance *d* in the linear path (3) from point C to point *D*. Finally, it transfers through the backward elliptical path (2) from point *D* to point *E*, where the path is repeated. In this tool path, the tool accomplishes both

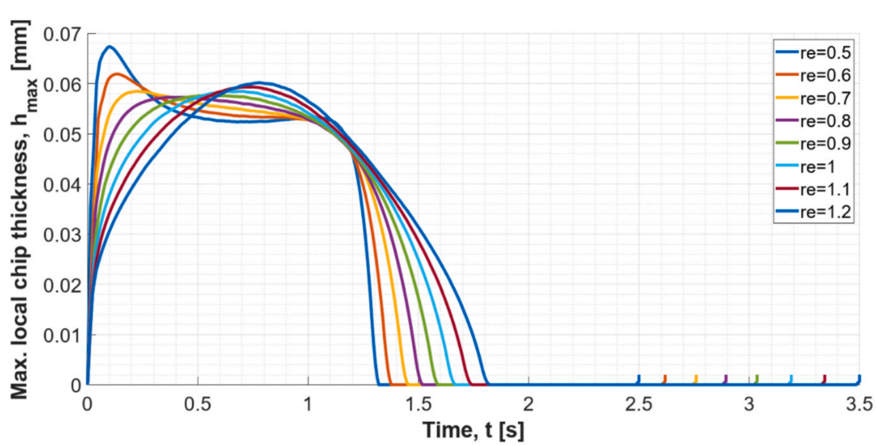

Fig. 7. Variation of the local maximum chip thickness, h_{max}, of elliptical tool path with time, t, for different aspect ratios, r_e, using conditions in Table 1.

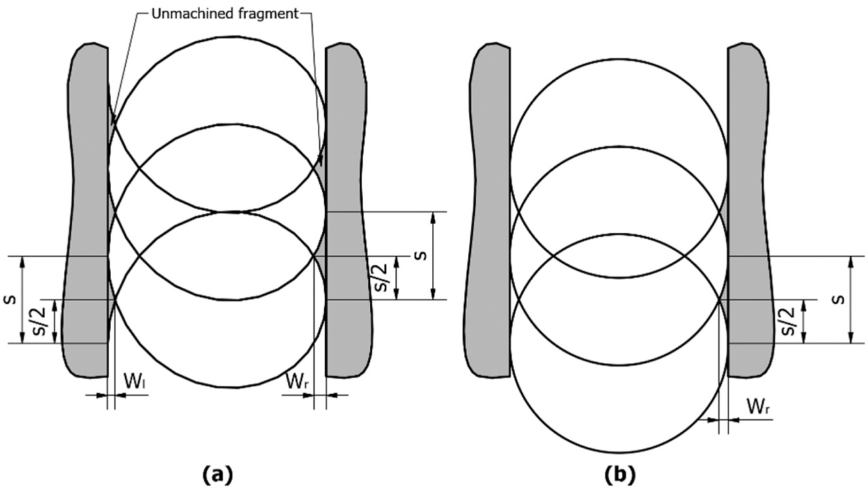

Fig. 8. Schematic drawing showing the waviness of the slot walls due to cutting tool motion in its path for (a) true trochoidal tool path and (b) circular-type trochoidal tool path.

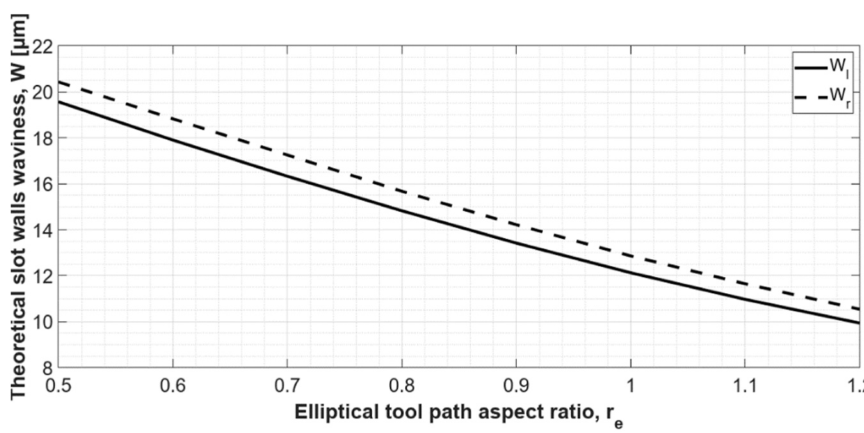

Fig. 9. The effect of elliptical tool path aspect ratio, r_e, on the slot left wall waviness, W_t, and the slot right wall waviness, W_r, using conditions in Table 1.

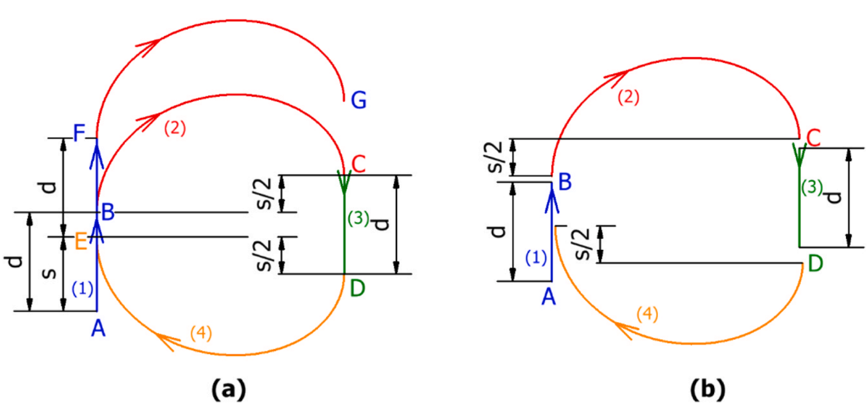

Fig. 10. The linear-elliptical tool path (a) and its four components (b).

conventional milling and elliptical trochoidal milling motions, where the tool performs conventional milling at the sides of the machined slot, decreasing the walls surface waviness and roughness, and elliptical trochoidal milling in between, improving the material removal rate and tool life. The method is a step toward combining roughing and finishing operation. The density of the tool imprints at the slot base is increased, improving the slot base surface roughness as well. By comparing the developed path with the elliptical path followed by a finishing path, it can be concluded that if the linear distance, *d*, is less than the trochoidal step, the tool path length of the developed path will be shorter. Hence, the material removal rate of the linear-elliptical trochoidal tool path will be larger, by using the same cutting conditions. On the other hand, the reduction of the linear distance will limit the improvement of the walls waviness and surface roughness.

3.1. *Effect of the linear-elliptical tool path on path length, walls waviness, and cooling time*

Although the insertion of linear paths into the elliptical path improves the slot walls texture, the tool path length increases, reducing the material removal rate. Hence, the linear distance, *d*, should be selected to reduce this side effect and achieve a proper development in the walls waviness and surface roughness. Fig. 11 demonstrates four linear-elliptical trochoidal tool paths of different linear distances. By increasing the linear distance, *d*, the waviness decreases, depending on the value of this distance, till this distance equals the trochoidal step, then the waviness is kept constant. As the linear distance equals or greater than the trochoidal step, the waviness depends on the feed per tooth instead of the trochoidal step. The waviness height at walls can be determined by substituting by (s-d)/2 in y_0 in Eq. (3) to find the value of x_0, to calculate the waviness at both. The relationships between the linear distance, *d*, of the linear-elliptical tool path and both the tool path length and the theoretical waviness of the slot walls, W, are illustrated in Fig. 12. The increase of the linear distance has a small effect on increasing the tool path length with a maximum increase of 4% at 1.2 linear distance, while the waviness reduces significantly by 98%. Therefore, the increase of the linear distance is effective in reducing the slot walls waviness until 0.85 s, where the waviness is not enhanced anymore.

4. Experimental work

Experimental work has been conducted to study the effects of the elliptical tool path on cutting forces, material removal rate, surface texture, and performance index. In addition, the effect of the linear-elliptical trochoidal tool path on improving surface texture and material removal rate will be studied.

Fig. 13 shows the equipment and measuring system used in the experiments. A square TiSiN-coated carbide endmill, from PAN TIGER (model of model P-SE1004 SI), has been used to machine a slot of 20 mm width, 20 mm length, and 6 mm depth in the workpiece using elliptical and linear-elliptical trochoidal tool paths with different aspect ratios as demonstrated in Table 4. The experiments have been conducted on DMG Mori ecoMill 600V CNC milling machine equipped by Siemens Sinumerik 840D. The machine tool is characterized by 12,000 rpm maximum speed, 20,000 mm/min maximum feed rate, and 1 μm table resolution in all directions. The tool used was 10 mm diameter of four cutting edges, and 35° helix angle. The tool extension length has been set to its minimum value, the flute length, 30 mm and it's fixed in all tests. The material of workpiece was P20 alloy steel in its unhardened state, which is used in molds manufacturing and other tooling applications due to its good mechanical properties and machinability. Its chemical composition is shown in Table 3. The workpiece was 60 mm width, 20 mm length, and 15 mm thickness.

The forces measuring system consists of a Kistler 4-component piezoelectric dynamometer of type 9272, a charge amplifier of type 5070A, and a data acquisition of type 5679A. The measuring ranges of the dynamometer were − 5:5 kN for the x and y directions and − 5:20 kN for the z direction. The total maximum sampling rate of the data acquisition is 10^6 samples/s for the four channels of the amplifier. The used sampling rate in the measurements was 10^4 samples/s. The arithmetic average value of the surface roughness, R_a, at the bottom and the walls of the machined slot, has been measured using Taylor-Hobson Surtronic 3 Roughness gauge of 0.01 μm resolution and 99.9 μm range. The bottom roughness has been measured in three places: beside the two slot walls and in the middle region of the slot. The cut-off distance has been selected to be 0.8 mm. The waviness height of the produced slot walls has been measured using Mitutoyo tool maker microscope of 1 μm resolution.

The experiments set arrangement is shown in Table 4, where the cutting conditions were kept constant, and only the elliptical tool path aspect ratio has been varied. The range of the aspect ratios 0.8–1.2 has been selected based on the low effect of these aspect ratios on the cooling time. The other cutting conditions have been selected based on preliminary experiments. Each experiment has been repeated three times. Additional three linear-elliptical trochoidal milling experiments have been conducted to study the effect of the linear distance *d* on material removal rate, waviness, surface roughness, and performance index. The distance *d*, as a function of the trochoidal step, has the values 0.75 s, s, and 1.25 s, where the trochoidal step equals 1 mm.

5. Results and discussion

5.1. *Cutting forces and material removal rate*

The measured forces in x, y, and z directions for the elliptical tool path of 0.8 aspect ratio and the circular tool path (r_e=1), using the conditions listed in Table 4, are shown in Fig. 14. The forces trends and values can be explained by the change of the tool-workpiece engagement value and position along the tool path. The curves consist of multiple tiny tooth-shaped curves due to the intermittent cutting nature of the milling process. The non-uniformities of the curves are due to the tool runout. There is no significant difference between the two curves in values but only the time of occurrence of the maximum force. For better clarification, the resultant cutting forces and their mean values are

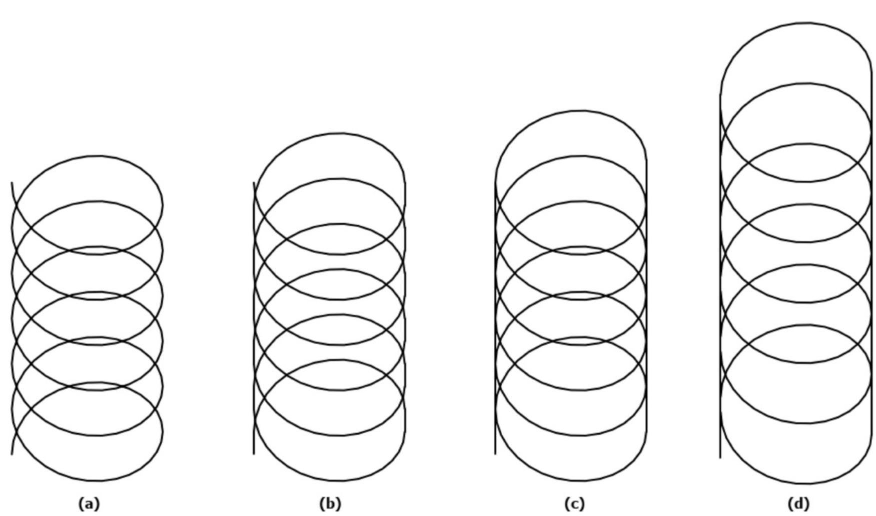

Fig. 11. Linear-elliptical tool paths of (a) d= 0, (b) d=s/2, (c) d=s, and (d) d= 1.25 s.

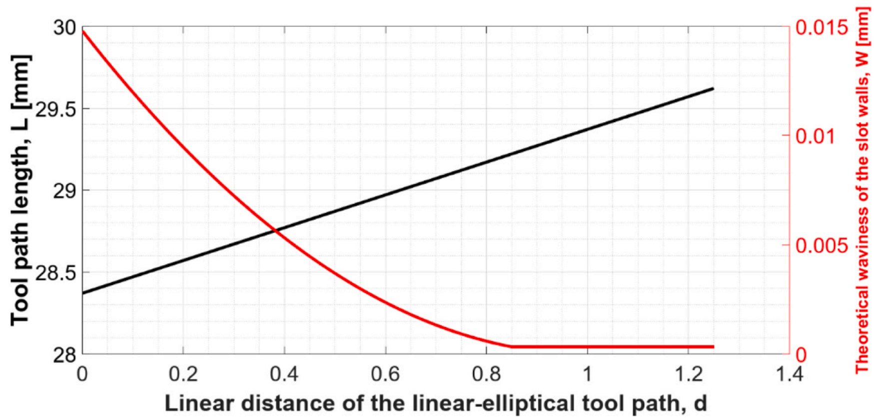

Fig. 12. Effects of the linear distance, d, of the linear-elliptical tool path on the tool path length, L, and the theoretical waviness of the slot walls, W, using the conditions in Table 1.

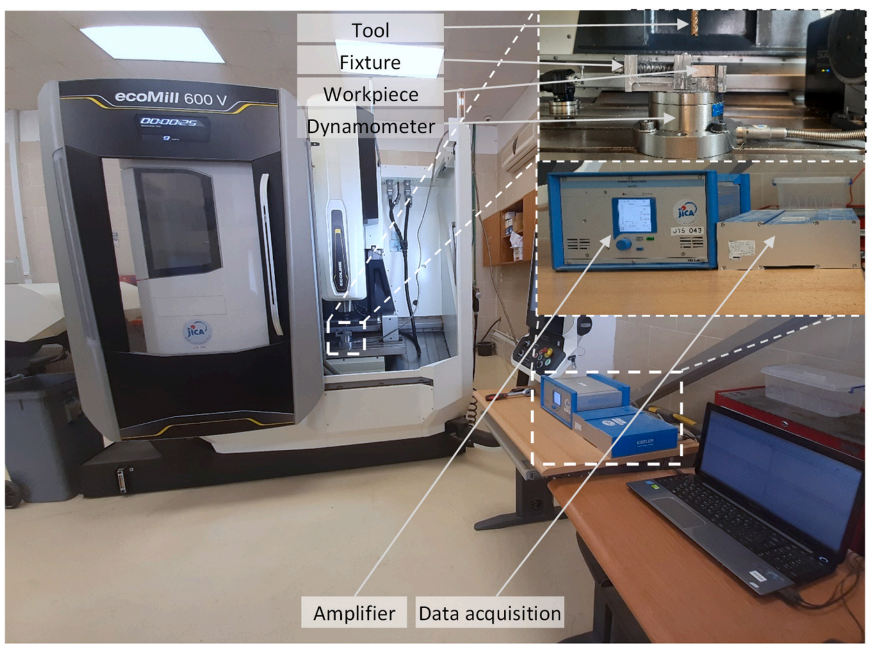

Fig. 13. Equipment and measuring system used in the experiments.

Table 3
Chemical composition of P20 steel alloy.

Element	C	Cr	Fe	Mn	Mo	P	S	Si	Other
Content (wt%)	0.374	1.8	95.6	1.44	0.259	0.0064	< 0.0005	0.299	< 0.07

Table 4
Process parameters used in the elliptical and linear-elliptical trochoidal milling experiments.

Parameter	Examined levels
Axial depth of cut, a_p [mm]	6
Tool center feed rate, f_r [mm/min]	600
Trochoidal step, s [mm]	1
Rotational speed, n [rpm]	2000
Elliptical tool path aspect ratio, r_e	0.8, 0.9, 1, 1.1, 1.2
Linear-elliptical tool path linear distance, d [mm]	0.75, 1, 1.25

displayed in Fig. 15. The resultant force increases to a maximum value then it diminishes. This trend is the same as the chip thickness variation along the tool path, Fig. 7. There is no significant difference between the values of maximum resultant forces in the two cases, but in the elliptical tool path, the force increases rapidly then it decreases slowly, while for the circular type, it increases and decreases at almost the same rate. The maximum force is attained after 9.7% and 16% of the cycle time from the start of the elliptical and circular tool paths respectively. This result is close to that of the chip thickness, where the maximum chip thickness occurred after 14.7% and 21.7% of the cycle time for the elliptical and the circular paths respectively.

Fig. 16 summarizes the effect of elliptical path aspect ratio, r_e, on the maximum resultant force, $F_{R,max}$, and the material removal rate, *MRR*. The aspect ratio of the elliptical tool path affects the material removal

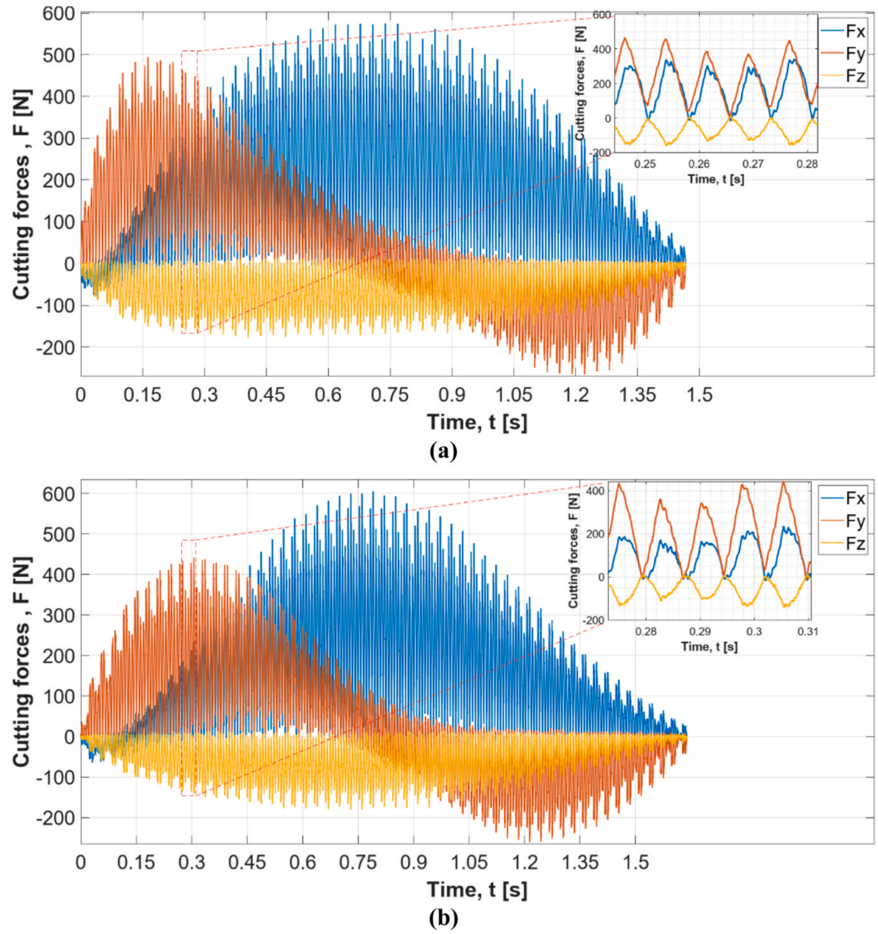

Fig. 14. The variation of cutting forces in x, y, and z directions with time for (a) elliptical tool path of 0.8 aspect ratio, r_e, and (b) circular tool path using the conditions listed in Table 4.

rate significantly, without a significant effect on the maximum resultant force (<3%). The decrease in aspect ratio from 1 to 0.8 increases the *MRR* by 11%, while it is reduced by 9% by increasing the aspect ratio to 1.2. These results are compatible with that of the chip thickness, where the chip thickness was not affected by the aspect ratio, while the material removal rate has been increased by 9%.

5.2. Surface texture

In this section, the surface texture of the produced slot by the elliptical trochoidal milling will be discussed. The waviness and surface roughness will be used as factors of surface texture evaluation. Fig. 17 shows the produced slot by elliptical trochoidal milling of 0.8 aspect ratio, where the machining marks due to the cutting tool rotation and feed are obvious on the slot bottom. The walls of the slot suffer from high waviness due to the lack of overlaps between successive tool revolutions.

5.2.1. Slot walls waviness

Fig. 18 demonstrates the experimental and the corresponding theoretical results of the left slot wall waviness, W_l, and that of the right one, W_r. The figure shows the consistency between the experimental and the theoretical results for the slot walls waviness with an error of less than 11%. The experimental results show that at low aspect ratios, 0.8 and 0.9, the left wall waviness is higher than that of the right wall, opposite to the theoretical results. This can be related to the increase of vibrations at the place of cutting tool direction change while the tool is performing machining. At low aspect ratios, the change of cutting tool direction is sharper than that at higher ratios. At higher ratios, the waviness of the left wall is slightly more than that of the right one. The walls waviness increases by decreasing the elliptical tool path aspect ratio. The elliptical tool path of 0.8 aspect ratio has a larger waviness by 45% than that of the circular one (r_e=1).

5.2.2. Slot surface roughness

Figs. 19 and 20 show the arithmetic average surface roughness, R_a, at the bottom and the walls of the machined slot by elliptical trochoidal milling at different aspect ratios, respectively. For the slot bottom, the surface roughness decreases significantly from left to right. These results can be explained by two main factors: the cutting tool imprints of overlapping successive revolutions at the slot base and the effects of the chip thickness on the tool forces and vibrations. In general, the average surface roughness over the slot bottom width, Fig. 19**,** is twice as low as at the slot walls, Fig. 20,. This was attributed to the increase of radial vibrations as compared to the axial vibrations and due to the high density of cutting edges imprints at the slot bottom due to the overlapping successive motion of the four cutting edges as it will be explained in Fig. 22.

Fig. 21 illustrates the imprints of four cutting edges of ten successive revolutions on the slot base. This figure has been constructed by drawing a circle representing the cutting-edge path in one tool rotation about its center and repeating it each feed per tooth distance along the tool path, forming the tool edges imprints. The local surface roughness value depends on the density of the tool imprints at the slot bottom. The density value is defined as the number of intersection points between the circular tool paths and the line X, which represents the measurement position in the x direction. As the tool imprints density increases, the

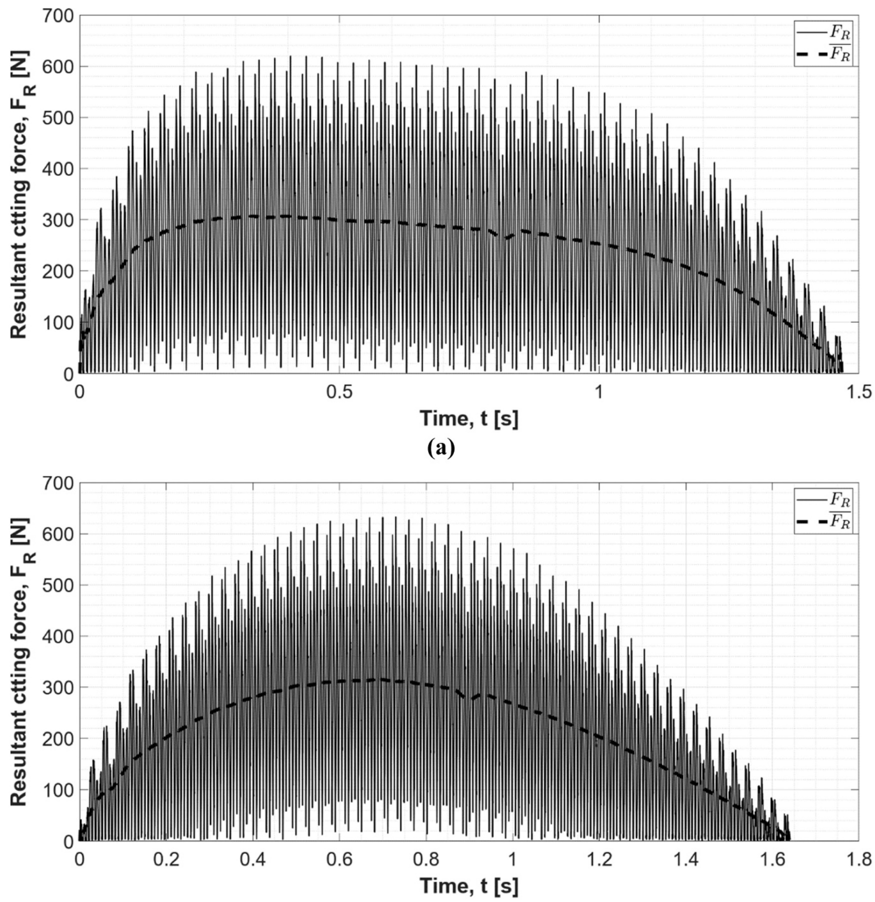

Fig. 15. The variation of resultant cutting forces and their means (dashed curve) with time for (a) elliptical tool path of 0.8 aspect ratio, r_e, and (b) circular tool path (lower figure) using the conditions listed in Table 4.

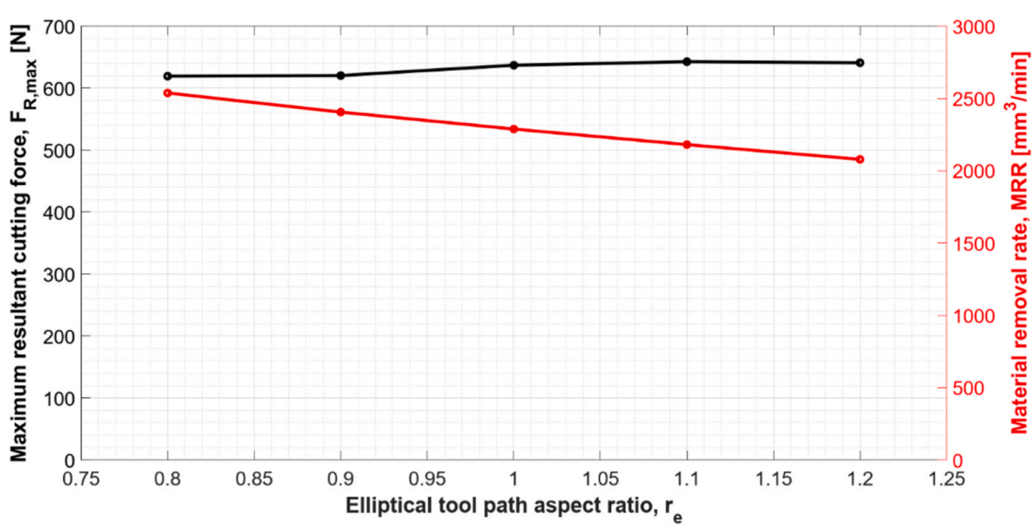

Fig. 16. Effect of the elliptical tool path aspect ratio, r_e, on the maximum resultant force, $F_{R,max}$, and the material removal rate, MRR.

surface roughness value decrease. Variation of the density of the cutting edges imprints from the left wall to the right wall is demonstrated in Fig. 22. The density of cutting edges imprints increases from the slot left wall to reach its maximum at the middle of the slot, then it decreases to zero at the right wall. This may explain why the surface roughness in the middle is smaller than that at the slot walls. Fig. 22 shows that the aspect ratio is not significant in affecting the imprints density.

By considering the relationship between the chip thickness and surface roughness. It can be observed that, at the right slot wall, the chip thickness is the lowest, Fig. 7, therefore the axial cutting forces and the induced vibrations are the lowest, consequently, the surface roughness is the lowest at this region. At the left of the slot, the surface roughness decreases considerably by increasing the aspect ratio, due to the reduction of the chip thickness, consequently, the axial cutting forces

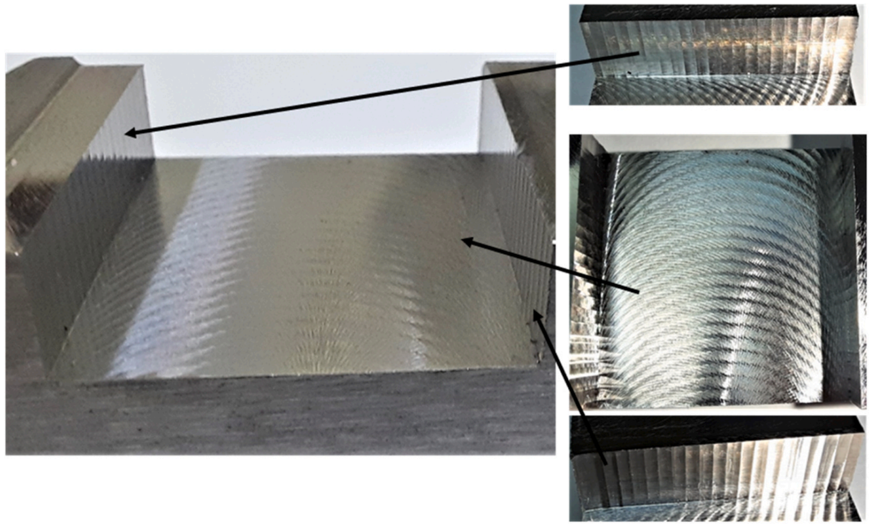

Fig. 17. The produced slot from elliptical trochoidal milling of 0.8 aspect ratio using the conditions listed in Table 4.

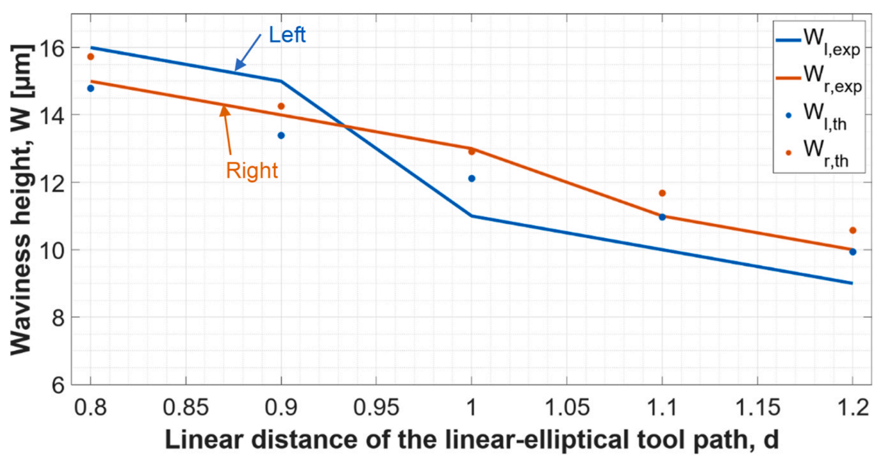

Fig. 18. The effects of the elliptical tool path aspect ratio, r_e, on the slot left wall waviness height, W_L, the slot right wall waviness height, W_R, and the corresponding theoretical values.

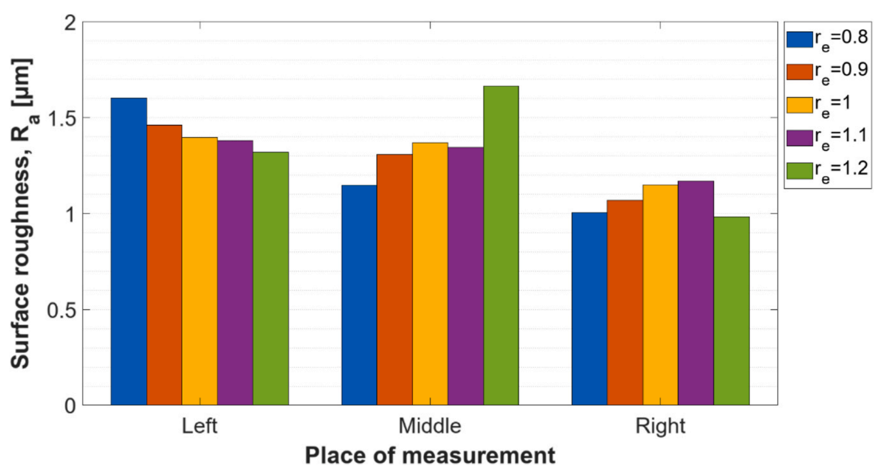

Fig. 19. Effect of elliptical tool path aspect ratio, r_e, on surface roughness, R_a, of the slot bottom at different places.

and the induced vibrations are reduced. In the middle and right of the slot, this arrangement is reversed, hence the surface roughness is increased by increasing the aspect ratio.

The surface roughness of the slot walls is almost double that of the bottom since the effects of the tool vibrations and runout are much larger in the transverse direction than that in the axial direction. The reduction of the surface roughness at the wall slot is attributed to the improvement of the tool motion smoothness and small vibrations

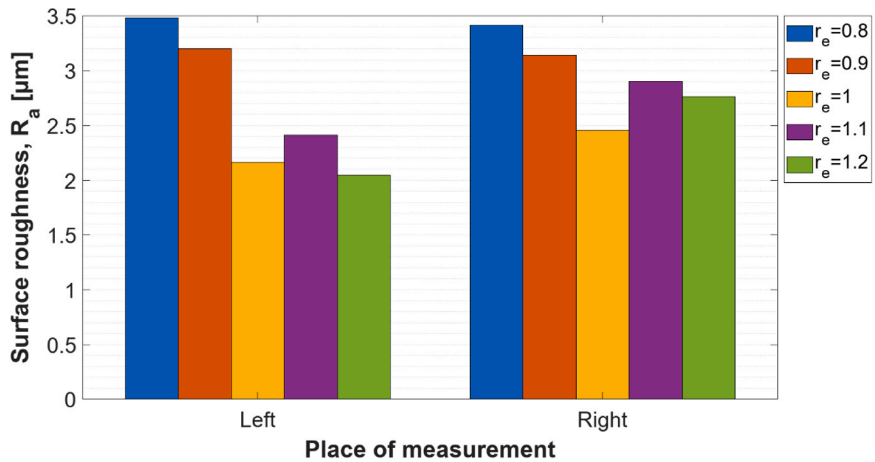

Fig. 20. Effect of elliptical tool path aspect ratio, r_e, on surface roughness, R_a, of the two slot walls.

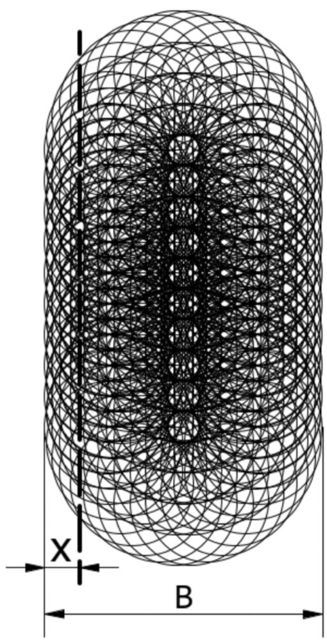

Fig. 21. Illustration of the cutting tool edges bottom imprints of ten successive revolutions for circular trochoidal tool path.

obtained due to high aspect ratio. For the elliptical paths of 1.1 and 1.2 aspect ratios, the surface roughness is more than the circular path increased due to the effect of the increased chip thickness. These results are compatible with that of Waszczuk et al. [12,25,26].

By comparing the surface roughness of the elliptical path with 0.8 aspect ratio and the circular path, it is found that the elliptical path produces higher roughness at the slot walls and the left bottom side than that of the circular one. As compared to the circular path, the slot left and right walls are rougher by 38% and 28% respectively, the left bottom side is rougher by 13%, while the middle and right side of the bottom are smoother by 19% and 14% respectively.

5.3. Performance Index

The elliptical tool path has different effects on the trochoidal milling, however, it improves the material removal rate, there are significant increases in the slot walls waviness and the surface roughness, while the cutting forces are almost the same. Therefore, in order to determine the performance of the elliptical tool path in trochoidal milling, a performance index will be utilized. The performance index, *PI*, can be defined as the ratio between the material removal rate to the multiplication of the maximum resultant cutting force, the maximum slot surface roughness, and the maximum slot waviness, Eq. (7). Fig. 23 illustrates the effect of the aspect ratio on the performance index. The circular tool path has better performance than the elliptical paths of 0.8 and 0.9 aspect ratios, however its reduced material removal rate. In comparison to the elliptical tool path, the circular tool path has a better performance by 45%. This increased performance is due to its lower waviness and surface roughness as compared to the elliptical paths. Hence, in order to improve the elliptical tool path, the waviness and surface quality should be enhanced. For this purpose, the linear-elliptical trochoidal tool path is proposed to improve waviness and surface quality, so the performance index can be enhanced.

$$PI = \frac{MRR}{F_{R,\max} R_{a,\max} W_{\max}} \tag{7}$$

Where (MRR) is the material removal rate, ($F_{R,\ max}$) is the maximum resultant cutting force, ($R_{a,max}$) is the maximum slot average surface roughness, and (W_{max}) is the maximum slot walls waviness.

5.4. Linear-elliptical tool path

Fig. 24 demonstrates the enhanced slot quality from linear-elliptical trochoidal milling of 0.8 aspect ratio and 1.25 mm linear distance, *d*. The produced walls are similar to that of conventional milling, i.e., less waviness and surface roughness. Figs. 25, 26, and 27 illustrate the positive effect of increasing the linear distance, *d,* on reducing the walls waviness, and bottom and walls surface roughness. Using the linear-elliptical tool path of linear distance 0.75 mm reduced the waviness three times as compared to the elliptical tool path, *d*= 0, while further increase improved it by only 60%. The surface roughness in the left and middle region of the bottom of the slot significantly decreased. The surface roughness of the left of the slot bottom has been decreased by 9%, 7%, and 16% for 0.75 mm, 1 mm, and 1.25 mm distance *d* respectively, while in the middle, it decreased by 8%, 26%, and 40% respectively. In the right region of the slot bottom, the surface roughness increased significantly. The reduction of surface roughness of the slot bottom can be explained by the increase of the cutting tool imprints. For slot walls, the surface roughness of the left side decreased by large ratios of 66%, 60%, and 68% for 0.75 mm, 1 mm, and 1.25 mm linear distance, *d,* respectively, while for the slot right wall, the reduction ratios are 61%, 72%, and 74% respectively. As shown, the waviness and surface roughness decreased significantly when the linear distance, *d*, equals 0.75 of the trochoidal step, then fewer reductions occurred by a further increase of this distance.

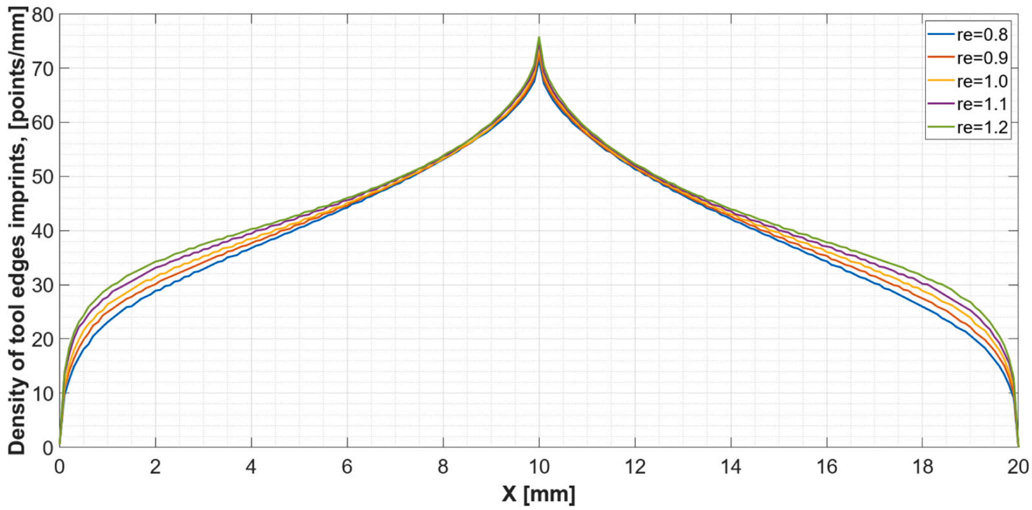

Fig. 22. Variation of the density of cutting edges imprints from the slot left wall to the slot right wall.

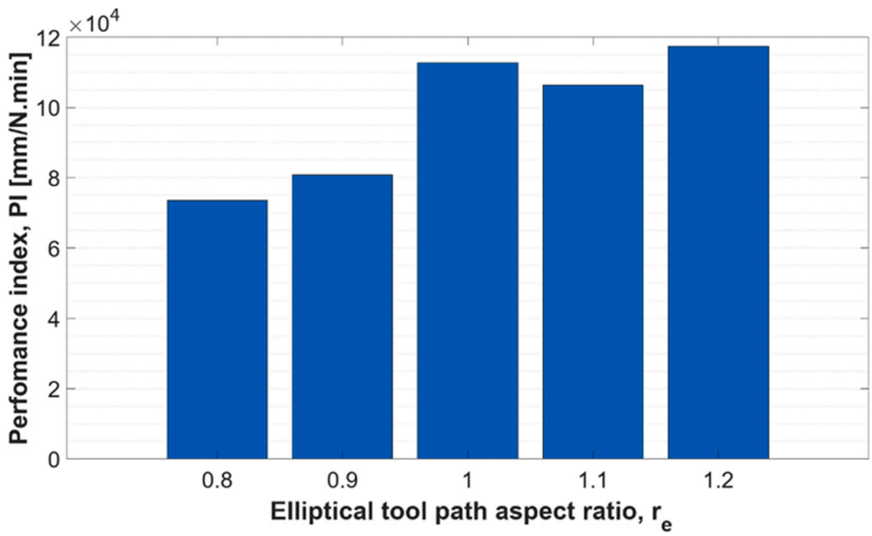

Fig. 23. Effect of the elliptical tool path aspect ratio, r_e, on performance index, PI.

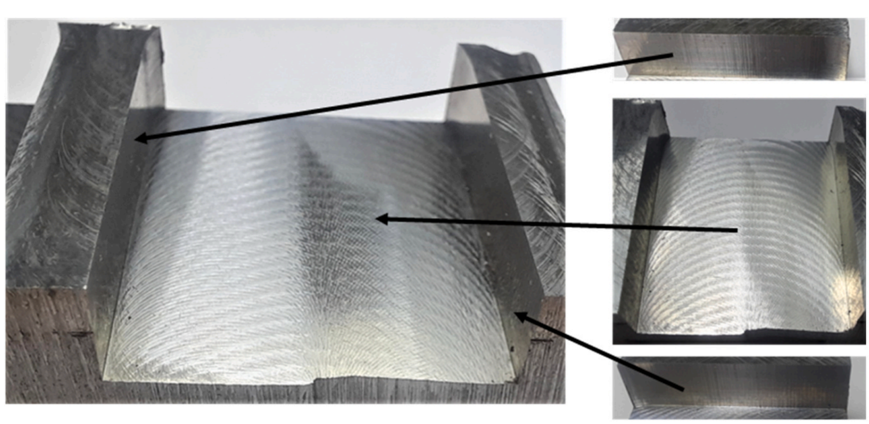

Fig. 24. The produced slot from linear-elliptical trochoidal milling of r_e= 0.8 and d= 1.25 mm.

However, the advantage of the linear-elliptical tool path in improving the surface texture, the material removal rate will be reduced due to the increase of the tool path. Hence the performance index will be used to evaluate this improvement concerning the process performance.

Fig. 28 reveals the effect of the linear distance, *d*, on material removal rate and performance index. The material removal rate has been decreased slightly by increasing this distance, where it decreased by 2.6%, 3.4%, and 4.2% for the distances 0.75 mm, 1 mm, and 1.25 mm

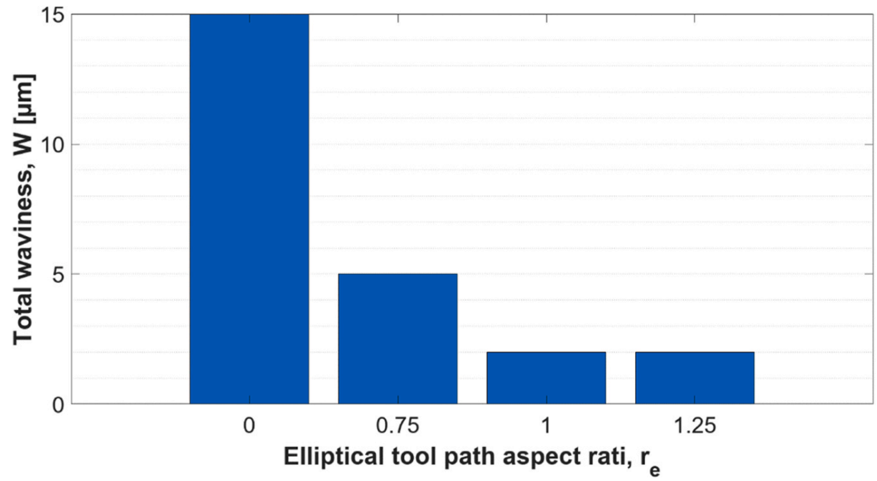

Fig. 25. Effect of the linear distance, d, of the linear-elliptical on the slot right wall waviness height, W at 0.8 aspect ratio.

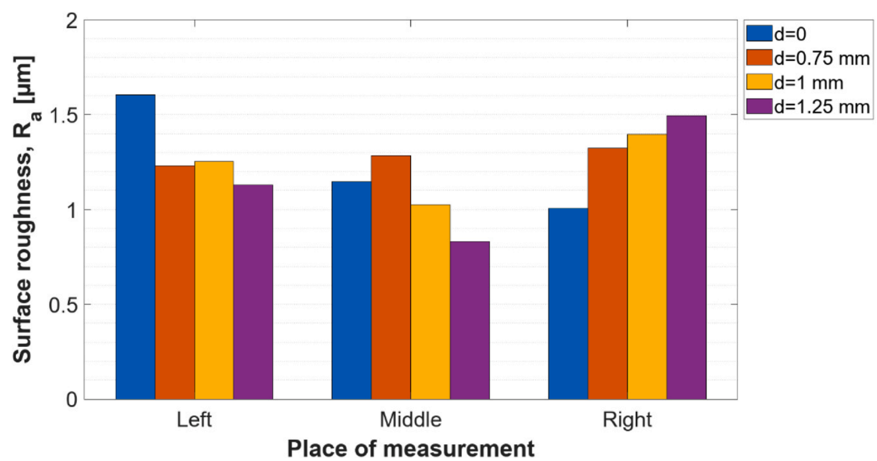

Fig. 26. Effect of increasing the linear distance, d, of the linear-elliptical on surface roughness, R_a, of the slot bottom at different places at 0.8 aspect ratio.

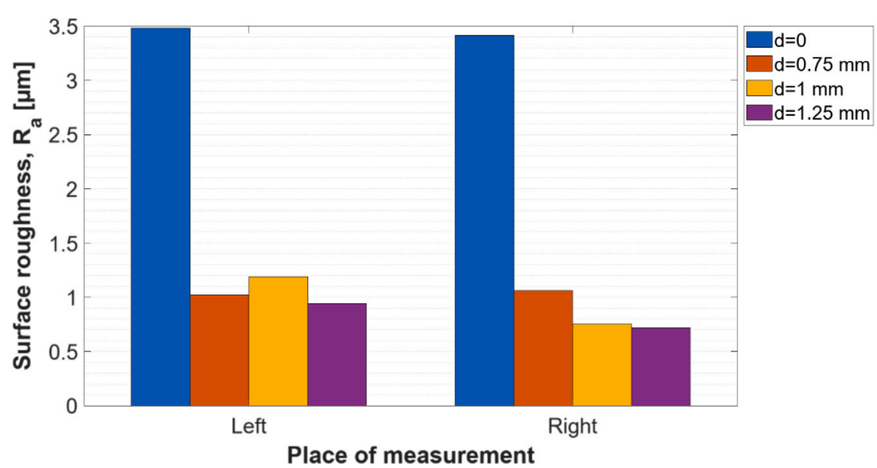

Fig. 27. Effect of the linear distance, d, of the linear-elliptical on surface roughness, R_a, of the slot walls at 0.8 aspect ratio.

respectively. The introduction of linear paths at the ends of the elliptical path increases the tool path length, consequently, a reduction in the material removal rate occurs. The performance has been improved greatly by 7.7, 18, and 16.7 times for 0.75 mm, 1 mm, and 1.25 mm linear distance respectively. Therefore, by comparing the elliptical and linear-elliptical tool paths, it is observed that the application of the developed linear-elliptical tool path improved the trochoidal milling performance by reducing the walls waviness and surface roughness significantly. By comparing the typical circular and linear-elliptical tool paths, it can be found that the linear-elliptical tool path has a larger material removal rate, enhanced surface quality, and better performance.

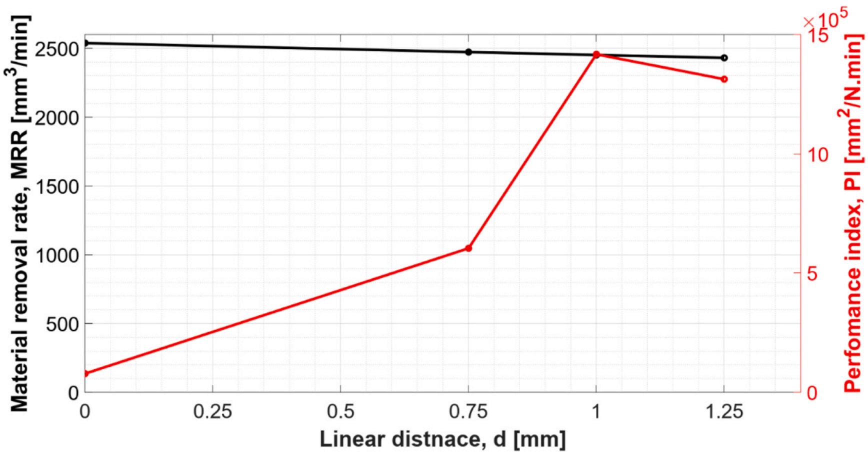

Fig. 28. Effect of the linear distance, d, of the linear-elliptical on material removal rate, MRR, and performance index, PI, at r_e= 0.8.

6. Conclusions

In this paper, the effects of the elliptical tool path on material removal rate, cutting forces, waviness, surface roughness, and performance index, in trochoidal milling, have been investigated. The linear-elliptical tool path has been proposed as a development of this elliptical path. The proposed path improved the performance of the trochoidal milling significantly by enhancing the material removal rate and reducing waviness and surface roughness. The following conclusions were obtained:

1) The application of elliptical tool path of 0.8 aspect ratio in trochoidal milling improves the material removal rate by 11% without a significant effect on cutting forces, however, it increases walls waviness and surface roughness by 36% and 38% respectively.
2) The reduction of elliptical path aspect ratio improves the material removal rate, but the walls waviness and surface roughness considerably increase with a slight effect on cutting forces.
3) The surface roughness of the machined slot walls in trochoidal milling is much more than that of its bottom.
4) In the developed linear-trochoidal tool path, the tool path combines linear and elliptical tool paths resulting in increasing the performance by about 18 times, the material removal rate by 5%, and the surface quality by 74%, with a slight reduction of the cutting forces in comparison to the circular tool path.
5) The increase of linear distance in the linear-elliptical tool path improves the waviness and surface roughness significantly, while the material removal rate is slightly reduced.

This study demonstrated that the linear-elliptical tool path has a significant influence on increasing trochoidal milling performance, which will contribute to the improvement of the process cost-effectiveness and machinability, however, a possible negative impact might be that when using this tool path; the tool cooling time will be decreased, increasing the tool wear. Hence, the cooling path effect requires more investigation in the future.

Funding

This research work is sponsored by the Egyptian Ministry of Higher Education (MoHE) grant and the Japanese International Cooperation Agency (JICA) in the scope of the Egypt-Japan University of Science and Technology.

CRediT authorship contribution statement

Mohamed Wagih: Conceptualization, Methodology, Validation, Formal analysis, Investigation, Data curation, Writing – original draft, Visualization. **Ibrahem Maher:** Conceptualization, Methodology, Validation, Formal analysis, Writing – review & editing, Visualization, Supervision. **Hassan El-Hofy:** Supervision. **Jiwang Yan:** Methodology, Writing – review & editing, Supervision. **Mohsen A. Hassan:** Conceptualization, Methodology, Validation, Formal analysis, Writing – review & editing, Visualization, Supervision.

Declaration of Competing Interest

The authors declare that they have no known competing financial interests or personal relationships that could have appeared to influence the work reported in this paper.

References

[1] Paulo Davim J. Machining of Hard Materials. London: Springer London; 2011.
[2] Grzesik W. Advanced Machining Processes of Metallic Materials. second ed. Elsevier; 2017.
[3] Amaro P, Ferreira P, Simões F. Comparative analysis of different cutting milling strategies applied in duplex stainless steel. Procedia Manuf 2020;vol. 47:517–24.
[4] Szalóki I, Csuka S, Csesznok S, Sipos S. Can trochoidal milling be ideal ?. Manufacturing 2012 The XXI. Conference of GTE on Manufacturing and related technologies. Hungary: Budapest; 2012.
[5] Rodríguez O, Romero PE, Molero E, Guerrero G. Advances in efficiency in the groove milling of aluminium EN AW 2024-T3 with zig-zag and trochoidal strategies. IOP Conf Ser Mater Sci Eng . 2021;vol. 1193(1):012005.
[6] Rodriguez-Alabanda O, Guerrero-Vaca G, Molero E, Romero PE. Experimental analysis of deep slot milling in EN AW 2024-T3 alloy by stretched trochoidal toolpath and variable helix angle tool. CIRP J Manuf Sci Technol 2021;vol. 35: 346–60.
[7] Sharif S, Ramli AS, Said AYM, Karim Z, Rahim EA, Sani ASA. Effect of cutting parameters on tool wear when trochoidal pocket milling Ti6Al4V. Int J Integr Eng 2019;vol. 11(4):159–65.
[8] Liu D, Zhang Y, Luo M, Zhang D. Investigation of tool wear and chip morphology in dry trochoidal milling of titanium alloy Ti–6Al–4V. Materials (Basel) . 2019;vol. 12 (12):1937.
[9] Amaro P, Ferreira P, Simões F. Tool wear analysis during duplex stainless steel trochoidal milling. AIP Conf Proc 2018;vol. 1960(1):070001.
[10] Pleta A, Nithyanand G, Niaki FA, Mears L. Identification of optimal machining parameters in trochoidal milling of Inconel 718 for minimal force and tool wear and investigation of corresponding effects on machining affected zone depth. J Manuf Process 2019;vol. 43:54–62.
[11] Shixiong W, Wei M, Bin L, Chengyong W. Trochoidal machining for the high-speed milling of pockets. J Mater Process Technol 2016;vol. 233:29–43.
[12] Waszczuk K, Skowronek H, Karolczak P, Kowalski M, Kołodziej M. Influence of the trochoidal tool path on quality surface of groove walls. Adv Sci Technol Res J 2019; vol. 13(3):38–42.
[13] Uddin MS, Matsubara A, Ibaraki S, Yasuda T. Comparison of cutting strategies for high productive end milling (no. mm) *Proc 35th Int MATADOR 2007 Conf* 2007: 191–4.

[14] Szalóki I, Csuka S, Sipos S. New test results in cycloid-forming trochoidal milling. Acta Polytech Hungarica 2014;vol. 11(2):215–28.
[15] Karkalos NE, Karmiris-Obratański P, Kurpiel S, Zagórski K, Markopoulos AP. Investigation on the surface quality obtained during trochoidal milling of 6082 aluminum alloy. Machines 2021;vol. 9(4).
[16] Prasad Patil JN, Polishetty Ashwin, Goldberg Moshe, Littlefair Guy. Slot machining of Ti6Al4V with trochoidal milling technique. J Mach Eng 2014;vol. 14(4).
[17] Santhakumar J, Mohammed Iqbal U. Parametric optimization of trochoidal step on surface roughness and dish angle in end milling of AISID3 steel using precise measurements. Materials (Basel) 2019;vol. 12(8).
[18] Otkur M, Lazoglu I. Trochoidal milling. Int J Mach Tools Manuf . 2007;vol. 47(9): 1324–32.
[19] Salehi M, Blum M, Fath B, Akyol T, Haas R, Ovtcharova J. Epicycloidal versus trochoidal milling-comparison of cutting force, tool tip vibration, and machining cycle time. Procedia CIRP 2016;vol. 46:230–3.
[20] Oh NS, Woo WS, Lee CM. A study on the machining characteristics and energy efficiency of Ti-6Al-4V in laser-assisted trochoidal milling. *Int J Precis Eng Manuf - Greening Technol* 2018;vol. 5(1):37–45.
[21] Huang X, Wu S, Liang L, Li X, Huang N. Efficient trochoidal milling based on medial axis transformation and inscribed ellipse. Int J Adv Manuf Technol 2020; vol. 111(3):1069–76.
[22] Jacso A, Lado Z, Phanden RK, Sikarwar BS, Singh RK. Bézier curve-based trochoidal tool path optimization using stochastic hill climbing algorithm. Mater Today Proc 2023.
[23] Hesterberg S, Albert B. Performance and limits of high-dynamic milling processes based on trochoidal tool paths. Acad J Manuf Eng 2017;vol. 15(4):107–11.
[24] García-Hernández C, Garde-Barace J-J, Valdivia-Sánchez J-J, Ubieto-Artur P, Bueno-Pérez J-A, Cano-Álvarez B, et al. Trochoidal milling path with variable feed. application to the machining of a Ti-6Al-4V Part. Mathematics . 2021;vol. 9(21): 2701.
[25] Waszczuk K, Karolczak P, Wisniewska M, Kowalski M. Influence of the path type on selected technological effects in the trochoidal milling. Adv Sci Technol Res J 2017;vol. 11(1):147–53.
[26] Waszczuk K. Influence of the trochoidal tool path generation method on the milling process efficiency. Adv Sci Technol Res J 2020;vol. 14(3):199–203.
[27] Wang QH, Wang S, Jiang F, Li JR. Adaptive trochoidal toolpath for complex pockets machining. Int J Prod Res 2016;vol. 54(20):5976–89.
[28] Wang Q-H, Liao Z-Y, Zheng Y-X, Li J-R, Zhou X-F. Removal of critical regions by radius-varying trochoidal milling with constant cutting forces. Int J Adv Manuf Technol . 2018;vol. 98:671–85.
[29] Deng Q, Mo R, Chen ZC, Chang Z. A new approach to generating trochoidal tool paths for effective corner machining. Int J Adv Manuf Technol . 2018;vol. 95: 3001–12.
[30] Jacso A, Matyasi G, Szalay T. The fast constant engagement offsetting method for generating milling tool paths. Int J Adv Manuf Technol 2019;vol. 103(9–12): 4293–305.
[31] Klocke, F. , Manufacturing Processes 1 – Cutting. 2011.
[32] Youssef HA, El-Hofy H. Machining technology: machine tools and operations. Mach Technol . 2008.
[33] A.I.H. Committee, *ASM Handbook, Volume 16: Machining*. ASM International, Electronic, 1989.
[34] Altintaş Y, Lee P. A general mechanics and dynamics model for helical end mills. CIRP Ann 1996;vol. 45(1):59–64.